
The following preprint has not yet undergone peer-review:
Hare, V.J. et al., *High-Precision Triple Oxygen Isotope Analysis of Carbon Dioxide by Tunable Infrared Laser Absorption Spectroscopy*.

Subsequent versions of this manuscript may have slightly different content. If accepted, the final version of this manuscript will be available via the 'Peer-reviewed publication DOI' link on the right hand side of this webpage. Please feel free to contact any of the authors; we welcome feedback.

July 10, 2022

High-Precision Triple Oxygen Isotope Analysis of Carbon Dioxide by Tunable Infrared Laser Absorption Spectroscopy

Vincent J. Hare,^{*,†,¶} Christoph Dyroff,[‡] David D. Nelson,[‡] and Drake A. Yarian[†]

[†]*Stable Light Isotope Laboratory, Department of Archaeology, University of Cape Town,
South Africa*

[‡]*Aerodyne Research Inc., Billerica, Massachusetts 01821, United States*

[¶]*ORCID: 0000-0002-4475-4109*

E-mail: vincent.john.hare@gmail.com

Phone: +27 (0)82 3333778

Abstract

Precision measurements of the stable isotope ratios of oxygen ($^{18}\text{O}/^{16}\text{O}$, $^{17}\text{O}/^{16}\text{O}$) in CO_2 are critical to atmospheric monitoring and terrestrial climate research. High-precision ^{17}O measurements by isotope ratio mass spectrometry (IRMS) are challenging because they require complicated sample preparation procedures, long measurement times, and relatively large samples sizes. Recently, tunable infrared laser direct absorption spectroscopy (TILDAS) has shown significant potential as an alternative technique for triple oxygen isotope analysis of CO_2 , although the ultimate level of reproducibility is unknown, partly because it is unclear how to relate TILDAS measurements to an internationally-accepted isotope abundance scale (e.g. VSMOW2-SLAP2). Here, we present a method for high-precision triple oxygen isotope analysis of CO_2 by TILDAS, requiring $\sim 8\text{-}9\ \mu\text{mol}$ of CO_2 (or 0.9 mg carbonate) in 50 minutes, plus ~ 1.5 hours for

sample preparation and dilution of CO₂ in N₂ to a nominal 400 μmol mol⁻¹. Overall reproducibility of Δ¹⁷O (CO₂) was 0.004 ‰ (4 per meg) for IAEA603 (SE, *n* = 6), and 10 per meg for NBS18 (SE, *n* = 4). Values corrected to the VSMOW2-SLAP2 scale are in good agreement with established techniques of high-precision IRMS, with the exception of Δ¹⁷O measured by platinum-catalyzed exchange of CO₂ with O₂. Compared to high-precision IRMS, TILDAS offers the advantage of ~ 10 times less sample, and greater throughput, without loss of reproducibility. The flexibility of the technique should allow for many important applications to global biogeochemical monitoring, and investigation of ¹⁷O anomalies in a range of geological materials.

The most commonly measured isotopologues of CO₂ are ¹²C¹⁶O¹⁶O, ¹³C¹⁶O¹⁶O, and ¹²C¹⁶O¹⁸O. Paleoenvironmental proxies based on these isotopologues (i.e. δ¹³C and δ¹⁸O) are widely used to reconstruct past climates, as well as to quantify the sources and sinks of CO₂, which are essential to understanding the global carbon budget. However, on their own these proxies are often insufficient, and additional constraints are needed to resolve carbon fluxes, past and present. Photochemical reactions during the formation of ozone are associated with mass-independent isotope effects which lead to anomalous enrichment in ¹⁷O in stratospheric CO₂.¹⁻⁴ The ¹⁷O enrichment is passed to the troposphere, and reset close to zero by mass-dependent isotopic exchange between CO₂ and the terrestrial biosphere (mostly leaves) and oceans.⁵ In terrestrial materials that contain oxygen, as well as the troposphere, the ¹⁷O anomaly (expressed as Δ¹⁷O)⁶ is a promising tracer for carbon exchange between reservoirs,^{2,5,7} as well as an exciting new proxy for paleoenvironmental change.⁸⁻¹¹ For the investigation of these effects, high-precision measurement (~0.01‰, or 10 per meg) of Δ¹⁷O is required, which is a challenging task for IRMS methods. These methods require the transformation of CO₂ to O₂ analyte, thereby avoiding isobaric interference between the ¹³C¹⁶O¹⁶O and ¹²C¹⁷O¹⁶O isotopologues, both of nominal mass 45. For this, various complicated techniques have been developed, including: conversion of CO₂ to O₂;^{9,12} isotopic exchange of subequal quantities of CO₂ and O₂ over a hot platinum catalyst;¹³⁻¹⁵ or by careful

equilibration of CO₂ with H₂O, and subsequent water fluorination to produce O₂.¹⁶

Recent advances in optical detection of rare isotopologues have led to a rapidly expanding array of applications to biogeochemistry, e.g. detection of radiocarbon dioxide at sensitivities approaching that of accelerator mass spectrometry;¹⁷ high-precision measurement of multiply-substituted isotopologues of both CH₄,¹⁸ and CO₂.¹⁹ The latter techniques all utilise tunable infrared laser direct absorption spectroscopy (TILDAS) for the direct measurement of isotopologue abundance ratios. Promisingly, Sakai *et al.*^{20,21} report TILDAS measurements of ¹⁸O/¹⁶O, ¹⁷O/¹⁶O from small quantities of CO₂ (2-68 μmol), with a precision of up to 30 per meg (SE, $n = 10$). The advantage of these methods over IRMS is that they require simpler laboratory procedures, and offer the potential of smaller samples sizes, and greater throughput. However, their overall reproducibility remains uncertain, and it is unclear how to relate TILDAS ¹⁸O/¹⁶O and ¹⁷O/¹⁶O ratios to commonly-used abundance scales, such as VSMOW2-SLAP2 or VPDB.

Here, we present a relatively simple method for triple oxygen isotope analysis by TILDAS which uses CO₂ evolved by acid digestion of interlaboratory carbonate reference standards, as well as a working reference gas, to produce high-precision Δ¹⁷O analyses, alongside δ¹³C. We have integrated TILDAS with an automated sample preparation system, which can also accept CO₂ from break-seal vials, acid digestion of ~ 0.9 mg of carbonate samples, or dry air from atmospheric flasks. The system ensures that CO₂ is well-mixed in N₂ prior to measurement, eliminating the possibility of isotope fractionation due to diffusion. We also present a framework for correcting spectroscopic ¹⁸O/¹⁶O and ¹⁷O/¹⁶O ratios to the VSMOW2-SLAP2 scale, and show that overall reproducibilities from TILDAS can match those of IRMS methods.

Experimental Section

Tunable Infrared Laser Direct Absorption Spectroscopy.

Our instrument is a commercial Aerodyne Research Inc. (ARI) tunable infrared laser direct absorption spectrometer (TILDAS).^{19,20,22} The instrument is based on the ARI dual-laser monitor platform, but is customized to the requirements of measuring CO₂ from carbonates, diluted to $\sim 400 \mu\text{mol mol}^{-1}$ in N₂. In the configuration presented here, the instrument enables the measurement of multiple isotopologues of CO₂ simultaneously. The instrument was equipped with two co-aligned distributed-feedback interband-cascade lasers (DFB-ICL, nanoplus Nanosystems and Technology GmbH). The ¹²C¹⁶O¹⁶O, ¹²C¹⁸O¹⁶O, and ¹³C¹⁶O¹⁶O isotopologues were targeted in the region of 2310 cm⁻¹, and the ¹²C¹⁷O¹⁶O isotopologue was targeted in the region of 2349 cm⁻¹. The wavelengths of the two lasers were chosen to achieve both strong and well-balanced absorption signals of the individual isotopologues of interest at the expected sample-isotopologue ratios.

The lasers and data acquisition were controlled by the ARI software TDLWintel, which also controlled the valve switching system (valves P9-P15 in Fig. 1), which is identical to the system reported elsewhere.¹⁹ Both lasers were scanned sequentially at a frequency of 1.5 kHz. Before analysis, 1500 spectra were averaged to achieve a 1-second average spectrum. This improved the signal-to-noise ratio by approximately $\sqrt{1500} = 38\times$. The averaged spectra were then individually fit to one spectroscopic model per laser. These models include: the relevant absorption lines of all isotopologues present in each spectral window; a baseline of a polynomial form; as well as the zero-light signal. The zero-light signal is equivalent to complete absorption, and the baseline is equivalent to no absorption (complete transmission).

Absorption signal enhancement was achieved by increasing the optical absorption path-length to 36 m using a multipass absorption cell. In this cell, the laser beams were reflected between two mirrors such that they accumulated 194 passes. Upon exiting the cell, the co-aligned beams were focused on a thermoelectrically cooled HgCdTe detector (J19, Teledyne

Judson). The sample pressure was around 28 Torr (10:1 reduction when expanding from volume 1, V1, in the valve switching system, previously filled via critical orifice through solenoid valves E1 (for sample gas) or E2 (for reference gas) see Fig. 1). The reduced pressure was used to sharpen the absorption lines and provide excellent isotopologue selectivity. This combined with the 36 m path length provided sufficient signal for very-high precision measurements.

Automated CO₂ Preparation System.

The automated CO₂ sample preparation system is designed to cryogenically purify, dilute, and mix sample CO₂ with N₂. Samples are able to be introduced to the system by any of 3 methods: loaded in break-seal tubes, from acid digestion of carbonates (via a Thermo GasBench II), or directly from a removable atmospheric sampling flask. Each sample introduction pathway is handled with a unique preparation sequence based in a custom LabVIEW program. The system consists of a break-seal manifold, liquid N₂ cryogenic trap, 3 mixing volumes (MV1, MV2, MV3 - combined volume 687 mL), and a circulation loop with inline diaphragm pump (CTS Series, Parker Hannifin Corp., USA) (Fig. 1). Valves 1-7, 16-21 are Swagelok SS4-BK-VA-1C bellows-sealed valves. V8 is a three-way solenoid valve (P/N 009-0294-900, Parker Hannifin Corp., USA). Non-numerically identified valves are manually toggled. Pressure gauges and corresponding data are handled by a data acquisition unit (cDAQ-9171, National Instruments Corp., USA). The sampling flask, which doubles as MV1, is custom made (GlassChem CC, South Africa, 576 mL) and designed to maximize turbulent mixing, see Supporting Information for photographs.

Samples are introduced from their respective source and first cryogenically trapped in MV2. After a short pump-over to promote purification and complete sample collection, CO₂ is thawed for 6 minutes and the yield measured (Agilent Varian CDG-500, 0-10 Torr). Sample yield is then used to calculate dilution and mixing requirements on a sample specific basis (target dilution is 400 $\mu\text{mol mol}^{-1}$) before being expanded into MV1. Ultra high-purity N₂

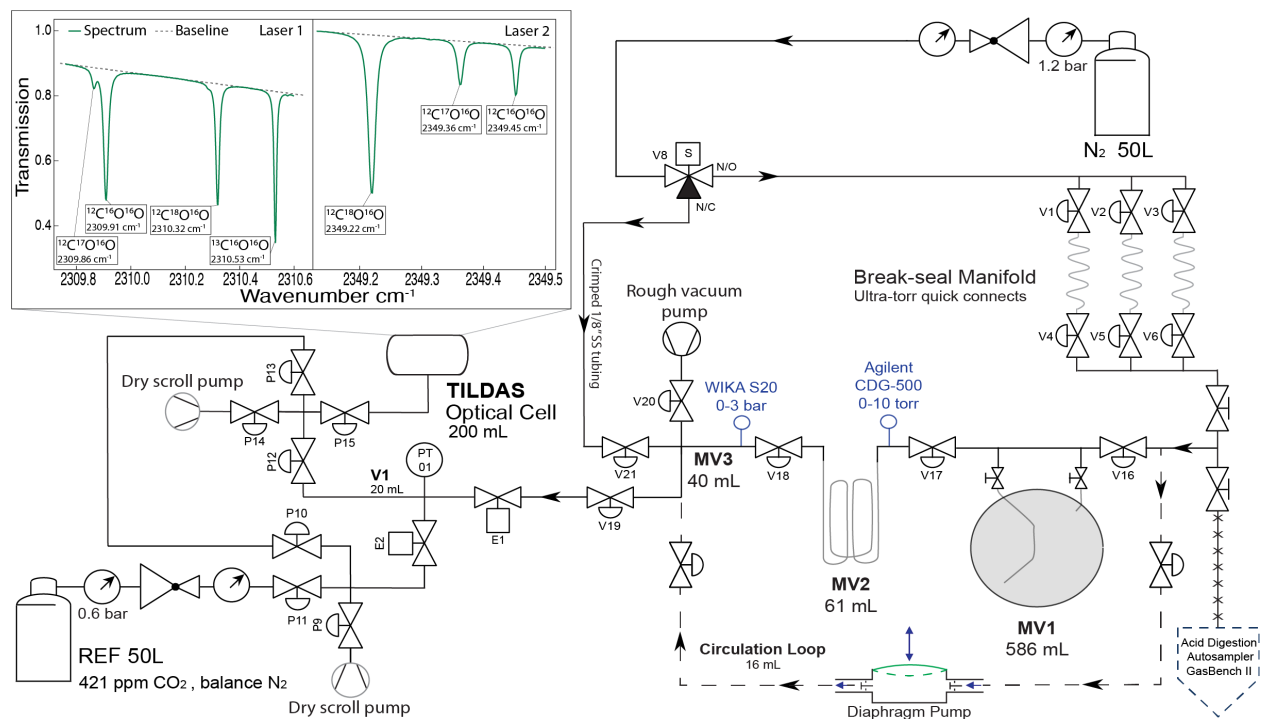


Figure 1: Schematic diagram of the system for automated preparation of CO₂ for high-precision TILDAS measurements of triple oxygen isotopes. MV1, MV2, and MV3 refer to mixing volumes 1 (586 mL), 2 (61 mL), and 3 (40mL). CO₂ from either acid digestion of carbonates (GasBench II) or alternatively, crackers, is frozen into MV2, and then diluted to $\sim 400 \mu\text{mol mol}^{-1}$ in N₂ in a specially-designed flask (MV1). The entire mixing volume (MV1,2,3) is then circulated for 2.5 minutes to ensure complete mixing prior to measurement. TILDAS sampling valves (pneumatic valves P9-P15, electronic valves E1 and E2) are the same as a previous system.¹⁹ Sampling valves allow for repeated comparisons between a 50L reference tank ($421 \mu\text{mol mol}^{-1}$ CO₂), and well-mixed sample in volume MV1,2,3.

as the diluent is regulated into the system at 1.2 bar and directed through a critical orifice, three-way solenoid valve, and crimped 1/8" stainless steel tubing into MV3 via valve V21. Dilution and initial mixing occur simultaneously as MV3 and MV2 are repeatedly pressurized with N₂ to 1450 mbar (WIKA S-20, 0-3 bar) and turbulently expanded into MV1. The exact number of repeated expansions is unique to each sample as calculated from the sample yield. See Supporting Information for detailed sequence summaries and mixing steps.

After dilution and initial mixing, samples are further mixed by opening the circulation loop and activating the diaphragm pump. Pump circulation is 750 mL min^{-1} , meaning that three complete circulations occur through MV1,2,3 in 2.5 minutes. After 2.5 minutes the

circulation loop closes and sample preparation is complete. Sample gas is then introduced to the TILDAS valve switching system via valve V19, a critical orifice, and valve E1. Sample pressures in the combined mixing volume typically begin around ~ 750 mbar and decrease to ~ 450 mbar over the course of an analysis. Overall repeatability of the sample concentration (evaluated from the $^{12}\text{C}^{16}\text{O}^{16}\text{O}$ isotopologue) was $403.6 \pm 8.2 \mu\text{mol mol}^{-1}$ (1σ , $n = 17$). Within sample (aliquot) concentration repeatability ranged from 0.4 to 0.9 $\mu\text{mol mol}^{-1}$ (1σ). Of importance to the success of our system are the high-precision Agilent Varian CDG-500 pressure gauge, sampling flask design, and circulation loop.

Reference Gas and Spectroscopic Measurement Procedure.

The reference used is a custom-made 50L high pressure cylinder of 421 $\mu\text{mol mol}^{-1}$ CO_2 in ultra high-purity N_2 (99.999%), made by Air Liquide South Africa (Pty) Ltd in July of 2021. The reference gas tank was allowed to sit for several months before initial measurements were made. Reference gas is regulated into the TILDAS at 0.6 bar using a sub-ambient high-purity absolute pressure regulator (3396 series, Matheson Tri-gas Inc., USA). Aliquots of reference gas are introduced via valve P11 (Fig. 1), a critical orifice, and valve E2 to an intermediate volume (V1, 20mL) all of which are part of the TILDAS sampling valve system, described elsewhere.¹⁹ Sub-ambient regulation of the reference gas is of critical importance as slowing the fill rate of V1 allows for greater accuracy in achieving the target fill pressure of 300 Torr, and therefore greater repeatability in optical cell pressure throughout an analysis. 0.6 bar is also comparable to sample filling pressures, promoting similar V1 filling accuracy between gases. Overall aliquot repeatability of the working reference gas concentration for the $^{12}\text{C}^{16}\text{O}^{16}\text{O}$ isotopologue was $421.4 \pm 0.4 \mu\text{mol mol}^{-1}$, evaluated over 12 hours of repeated measurement (1σ , $n = 148$).

All aspects of the TILDAS measurement system, (e.g. timings, laser control, data acquisition, signal processing, etc.) are controlled by dedicated software (TDLWintel). Analyses are performed by repeatedly alternating aliquots of sample and reference gas into the TILDAS,

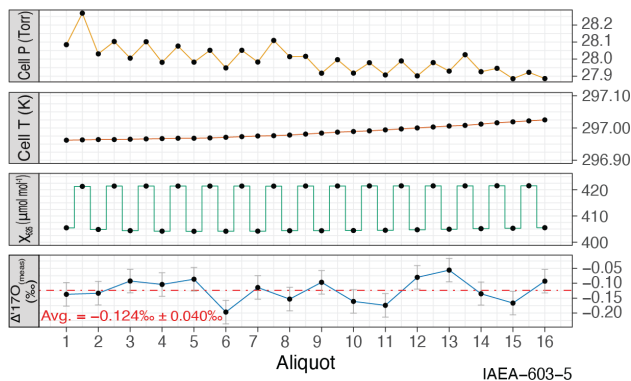


Figure 2: TILDAS measurement procedure. Repeated comparisons between a 50L reference tank ($421 \mu\text{mol mol}^{-1} \text{CO}_2$), and well-mixed sample of $8.645 \mu\text{mol CO}_2$, evolved from 0.914 mg of IAEA603 carbonate, by phosphoric acid digestion (70°C for 2 hours) and mixed to $404.8 \mu\text{mol mol}^{-1}$ in N_2 (703.53 mbar total sample). The measurement sequence takes around 50 minutes. Optical cell temperatures and pressures during this time were stable to within $<0.1 \text{ K}$ and $<300 \text{ mTorr}$, respectively. Laboratory temperature variations were no more than $0.11 \text{ }^\circ\text{C min}^{-1}$. 16 aliquots were averaged in total. χ_{626} is concentration of the $^{12}\text{C}^{16}\text{O}^{16}\text{O}$ isotopologue. Error bars for $\Delta^{17}\text{O}_{\text{meas}}$ are 1σ .

analogous to dual-inlet IRMS methods. This is done by filling V1 to 300 Torr of either sample or reference gas, followed by expansion into the pre-evacuated optical cell (200 mL). Each aliquot is measured in the optical cell for 40 seconds, during which the next aliquot is filled into V1, before being evacuated and the next introduced. A measurement cycle, defined as the measurement of subsequent aliquots of sample and reference gas, takes ~ 3 minutes. Optical cell pressure is typically $\sim 28 \text{ Torr}$, and generally stable to $<300 \text{ mTorr}$. Cell temperature is typically $\sim 297 \text{ K}$ and stable within 0.1 K (Fig. 2). A complete analysis, typically comprising of 18-20 measurement cycles, takes around 50 minutes. For all analyses, the first 3 measurement cycles are ignored due to stabilization of temperature within the optical cell.

From 31 March to 5 April lab aircon control malfunctioning was noted. During this period it was identified that poor $\Delta^{17}\text{O}$ precision was correlated to the rate of change of TILDAS electronics temperature (dT/dt). Samples analyzed between these dates were excluded as the amplitude of dT/dt ($A(dT/dt)$) was greater than $0.11 \text{ }^\circ\text{C min}^{-1}$, as evaluated by a 200-second moving average. All other samples as reported in this study showed $A(dT/dt) < 0.11$

°C min⁻¹ (see Supporting Information for further analysis of this effect).

Results and Discussion

Definition of Spectroscopic δ -values, and Concentration Dependence due to Scale-Offset Error.

Optical isotope spectrometers, such as our TILDAS instrument, determine δ -values by measuring mole fractions of isotopologues.²³ Adopting IUPAC notation,^{24,25} we can write, e.g. for the ¹²C¹⁷O¹⁶O isotopologue:

$$\delta^{17}\text{O}_{\text{meas}} = \left(\frac{\chi_{627}/\chi_{626}}{X_{627}/X_{626}} - 1 \right) \times 1000 , \quad (1)$$

where the mole fraction, $\chi_{627} = C_{627}V/n$, is related to the measured concentration (C) of the ¹²C¹⁷O¹⁶O isotopologue in the optical cell (of volume, V). Similar expressions can be derived for other isotopologues. X is the isotopologue abundance ratio (mol mol⁻¹) as specified in the high-resolution transmission molecular absorption database (HITRAN), a standard database of *ab initio* atmospheric simulations.²⁶ In eq. (1), χ is analogous to the isotope ratio of the sample, e.g. (¹⁷O/¹⁶O)_{sample}, in the usual definition of an IRMS δ -value, and X is analogous to the isotope ratio of the standard, (¹⁷O/¹⁶O)_{std}. A δ -value measured by spectroscopy (eq. 1) is thus not relative to a scale such as VPDB or VSMOW2-SLAP2, but rather, relative to HITRAN. Briefly, we also note that a spectroscopic δ -value is technically a molecular abundance ratio, and not an atomic abundance ratio, as is measured by IRMS. However, it is assumed (for now) that the difference between the two is negligible.²⁷

Because δ -values measured by TILDAS are relative to HITRAN abundances, an extra step is needed to convert them to the VSMOW2-SLAP2 scale. A conversion procedure has previously been outlined to correct spectroscopic $\delta^{13}\text{C}_{\text{meas}}$ for the offset from the VPDB scale.²³ We extend this procedure to the triple oxygen isotope system (and VSMOW2-

SLAP2) as follows. Adopting the notation $\chi'_{627} = \chi_{627}/X_{627}$, we can modify eq. (1) thus:

$$\delta^{17}\text{O}_{\text{meas}} = \left(\frac{a_{627}\chi'_{627} + b_{627}}{a_{626}\chi'_{626} + b_{626}} - 1 \right) \times 1000 , \quad (2)$$

where a_{627} , b_{627} , a_{626} , and b_{626} are scale factors which relate the HITRAN mole fractions to the equivalent mole fractions on VSMOW2-SLAP2. Assuming $A_{627} = a_{627}/a_{626}$, and dropping the factor of 1000 for convenience, with further modification it can be shown²³ that:

$$\delta^{17}\text{O}_{\text{std}} = \frac{\chi'_{626}}{A_{627}(\chi'_{626} - b_{626})} \left[\delta^{17}\text{O}_{\text{meas}} + \frac{(A_{627}b_{626} - b_{627})}{\chi'_{626}} - A_{627} + 1 \right] . \quad (3)$$

This provides a general equation to correct TILDAS δ -values to the VSMOW2-SLAP2 scale. For interlaboratory carbonate standards, the value of $\delta^{17}\text{O}_{\text{std}}$ is assumed (or is measured by IRMS), and $\delta^{17}\text{O}_{\text{meas}}$ and χ_{626} are both then measured by TILDAS on multiple samples of CO_2 evolved from e.g. NBS18 and IAEA603 (mixed with dry N_2). The constants A_{627} , b_{627} , and b_{626} are then determined by non-linear least squares fitting to eq. (3). The same procedure is then performed to correct $\delta^{18}\text{O}_{\text{meas}}$ to $\delta^{18}\text{O}_{\text{std}}$ (with constants A_{628} , b_{628} , and b_{626}). Note that if $A_{627} = 1$ and $b_{627}, b_{626} = 0$, then eq. (3) reduces to $\delta^{17}\text{O}_{\text{std}} = \delta^{17}\text{O}_{\text{meas}}$, and the two scales are equal, as expected.

Significantly, eq. (3) shows that uncorrected TILDAS δ -values will depend on the measured concentration of the most abundant $^{12}\text{C}^{16}\text{O}^{16}\text{O}$ isotopologue (χ'_{626}). We call this effect a “*concentration dependence due to scale-offset error*”, because it arises purely as an arithmetic consequence of the definition of the δ -value (eq. 1), and the offset between HITRAN and VSMOW2-SLAP2 isotopologue abundance scales.

Isotope Effects due to Diffusion of CO_2 During Sample Preparation.

Our TILDAS protocol requires highly-repeatable dilutions of CO_2 in N_2 to trace concentration. This is because dilution in N_2 broadens the isotopologue absorption lines, and minimises the spectral baseline, thereby increasing measurement precision. However, if dilution

is incomplete, and the sample is not very well mixed, isotope fractionation due to diffusion will be reflected in $\delta^{17}\text{O}_{\text{meas}}$ and $\delta^{18}\text{O}_{\text{meas}}$ values, in addition to concentration dependence (described above). Diffusion effects were found to be negligible in TILDAS measurements of the clumped isotopologue $^{13}\text{C}^{16}\text{O}^{18}\text{O}$ (CO_2 in N_2 at 0.35%), due to cancellation of factors in the equation for the clumped equilibrium constant, K .¹⁹ However, diffusion is likely to be more important in the triple oxygen isotope system, where very small differences in $\delta^{17}\text{O}$ and $\delta^{18}\text{O}$ propagate into large errors in $(\Delta^{17}\text{O})$.⁶

For triple oxygen isotopes, the relationship between fractionation factors during diffusion is defined⁶ as $\alpha^{17/16} = (\alpha^{17/16})^\theta$, which, rearranging, gives:

$$\theta_{\text{diff}} = \frac{\ln(\alpha^{17/16})}{\ln(\alpha^{18/16})}. \quad (4)$$

Where the subscript ‘‘diff’’ indicates a diffusion process. For diffusion of CO_2 in N_2 , the binary diffusion coefficient can be calculated from Chapman-Enskog theory using:

$$D_{ab} = \frac{AT^{3/2}}{p\sigma_{ab}^2\Omega} \sqrt{\frac{m_a + m_b}{m_a m_b}}. \quad (5)$$

The subscripts a and b refer to the two gases, m is the molecular mass of each gas, and σ and Ω are the average collision diameter (4.15 Å) and temperature dependent collision integral (~ 1), respectively. At 21 °C and 700 mbar, D is 0.1879 $\text{cm}^2 \text{s}^{-1}$. Eq. (5) can be modified to describe the ratios of isotopologue concentrations, and thereby related to fractionation factors. With further algebra, common terms such as T , p , etc. will cancel, and it can be shown that the ratio of fractionation factors is just the ratio of diffusivities for

each isotopologue:

$$\begin{aligned}
\theta_{\text{diff}} &= \frac{\ln\left(\frac{D_{45,28}}{D_{44,28}}\right)}{\ln\left(\frac{D_{46,28}}{D_{44,28}}\right)} \\
&= \frac{\ln\left(\frac{44}{45}\right) + \ln\left(\frac{45+28}{44+28}\right)}{\ln\left(\frac{44}{46}\right) + \ln\left(\frac{46+28}{44+28}\right)} \\
&= 0.509
\end{aligned}$$

According to the conventional δ -notation definition of the triple oxygen isotope system,

$$\Delta^{17}\text{O} \equiv \delta^{17}\text{O} - \theta\delta^{18}\text{O} , \quad (6)$$

where $\theta = 0.528$ (global reference line) and $\delta^{17}\text{O} = 1000\ln(\delta^{17}\text{O}/1000 + 1)$, and a similar expression exists for $\delta^{18}\text{O}$. Hence, the mass-dependent fractionation exponent, θ , is lower for diffusion than for the global reference line. When CO_2 diffuses in N_2 , $\delta^{18}\text{O}$ and $\delta^{17}\text{O}$ values will be shifted lower relative to their original values (i.e. relative to the pure CO_2). This gas will also tend to be under-diluted with respect to the target concentration ($400 \mu\text{mol mol}^{-1}$). And by mass balance, $\delta^{18}\text{O}$ and $\delta^{17}\text{O}$ values of the remaining (un-mixed) CO_2 will be shifted higher.

A framework for errors due to diffusion, as well as scale-offset, are shown in Fig. 3A for a hypothetical gas with a true value of $\Delta^{17}\text{O}_{\text{meas}} = 0$. If the sample gas is well-mixed, with no diffusion, and no offset error, then all aliquots would be measured along a line of slope $\theta = 0.528$ in $\delta^{17}\text{O}_{\text{meas}}-\delta^{18}\text{O}_{\text{meas}}$ space. Samples with scale-offset error would lie along a curve (shown in red) depending on the measured concentration of $^{12}\text{C}^{16}\text{O}^{16}\text{O}$ (χ'_{626} , eq. 3), as well as the values of A_{627} , A_{628} , etc. In addition, if there are diffusion effects, then individual aliquots will lie along a slope of $\theta = 0.509$ (shown in blue). In reality, the two effects occur together, so that the total error, $\varepsilon(\Delta^{17}\text{O})$, is the sum of errors due to scale offset, $\varepsilon(\text{scale})$, and diffusion, $\varepsilon(\text{diff})$. Aliquots of higher concentration will be found above the true slope, and lower concentrations below it, resulting in a ‘‘cone’’ of scatter, with an average gradient

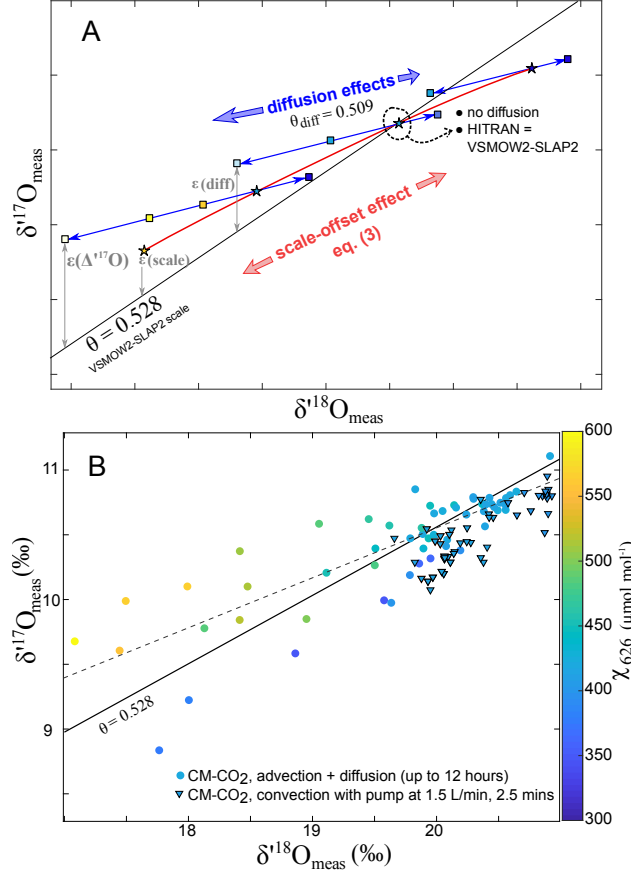


Figure 3: (A) Graphical framework for errors in TILDAS measurements of triple oxygen isotope composition of CO_2 (see further discussion in text). Stars are samples of different target concentration. Squares are aliquots drawn from each sample (under- or over-diluted). (B) shows the effects of incomplete mixing of CO_2 in N_2 on $\delta^{17}\text{O}_{\text{meas}}$ and $\delta^{18}\text{O}_{\text{meas}}$. Filled triangles show multiple aliquots from 4 samples of CO_2 evolved from an internal standard, Cavendish Marble (CM), circulated by diaphragm pump (Parker CTS) for 2.5 minutes to allow proper mixing before measurement. Other datapoints are aliquots from five samples of CM, mixed only by advection and diffusion (for up to 12 hours).

lower than $\theta = 0.528$ (and erroneously high $\Delta^{17}\text{O}_{\text{meas}}$ values).

To test this framework, we conducted an experiment on samples with and without our circulating pump, using CO_2 from ~ 0.8 mg samples of an internal laboratory standard, Cavendish Marble (CM- CO_2). 5 samples were mixed into MV1,2,3 by turbulent advection and diffusion only, without the circulating pump. The time taken for diffusive mixing was varied on a sample-by-sample basis from ~ 10 minutes to 12 hours. In addition, the average χ'_{626} of each sample varied from 400 to 466 $\mu\text{mol mol}^{-1}$. 4 samples of the same material were

mixed for ~ 2.5 minutes with the pump, immediately after turbulent advection. χ'_{626} of these samples varied from 368 to 405 $\mu\text{mol mol}^{-1}$.

For the samples unmixed by pump, Fig. 3B shows good agreement with the framework in Fig. 3A. Aliquots from all samples form a cone of scatter, with an average slope (dashed line) lower than $\theta = 0.528$. Better-mixed aliquots, close to the target concentration range, cluster more closely to $\theta = 0.528$. When the circulating pump is added (filled triangles), all aliquots have an average slope very near $\theta = 0.528$. Without the pump, 1σ sample repeatability for $\Delta^{17}\text{O}_{\text{meas}}$ was 30 ± 130 per meg, and aliquot repeatability for χ'_{626} was between 4 and 80 $\mu\text{mol mol}^{-1}$. With the pump, sample repeatability for $\Delta^{17}\text{O}_{\text{meas}}$ improved substantially to -230 ± 10 per meg, in significantly less time (~ 2.5 minutes vs hours). With the pump, aliquot repeatability for χ'_{626} was also excellent. This result supports the conclusion that, without proper mixing, diffusion effects can be very significant in TILDAS measurements of $\Delta^{17}\text{O}$, necessitating very long times for well-mixed samples measurement (further discussion of diffusion times in Supporting Information). Promisingly, forced convection via circulating loop solves these issues. Preparation of the entire sample gas prior to measurement (as opposed to aliquot-by-aliquot basis) also provides a useful check on the extent of mixing, which may be evaluated by aliquot repeatability of χ'_{626} .

Correction of Spectroscopic $\delta^{17}\text{O}$ and $\delta^{18}\text{O}$ values to the VSMOW2-SLAP2 Scale.

In what follows, we compare triple oxygen isotope measurements both without correction ($\delta^{17}\text{O}_{\text{meas}}$, $\delta^{18}\text{O}_{\text{meas}}$), and corrected to VSMOW2-SLAP2 ($\delta^{17}\text{O}_{\text{corr}}$, $\delta^{18}\text{O}_{\text{corr}}$). These data are shown in Table 1. All samples were well-mixed by circulating pump for 2.5 minutes prior to TILDAS measurement (described in detail above). For conciseness, corresponding $\delta^{13}\text{C}$ data for these samples are reported in the Supporting Information. For the correction, we used interlaboratory carbonate standards IAEA603 ($n = 6$), and NBS18 ($n = 4$). Assuming VSMOW2-SLAP2 values for CO_2 from IAEA603 and NBS18 given by Wostbrock *et al.*,¹² we

fitted eq. (3) to all aliquots of $\delta^{17}\text{O}_{\text{meas}}$, and χ'_{626} , in MATLAB. The same procedure was then performed for $\delta^{18}\text{O}_{\text{meas}}$. For $\delta^{17}\text{O}$, the fitted parameters were: $A_{627} = 0.674$, $b_{627} = -1974$, $b_{626} = -168$, $R^2 = 0.999$; and for $\delta^{18}\text{O}$, they were $A_{628} = 0.632$, $b_{628} = -3782$, $b_{626} = -207$, $R^2 = 0.999$.

We have corrected our δ -values to the VSMOW2-SLAP2 scale using previously-published values for carbonate standards from an IRMS method¹² because this particular method is regarded as a relatively assumption-free for triple oxygen isotope analysis.²⁸ A more nuanced approach, for future investigation, would be to perform equilibrations between CO_2 and VSMOW2, SLAP2 water directly on our cart within MV3, thereafter trapping and analyzing the equilibrated CO_2 . Another alternative is to correct our working reference gas directly to VSMOW2-SLAP2.²³ In our procedure, we avoid calibrating our working reference gas because (1) it is used merely to correct for short-term drift in δ -values between aliquots, and (2) because long-term drift might occur as our 50L tank empties (for instance, due to potential effusion effects).

Although we also report NBS19 ($n = 7$) in this table, it was excluded from the fitting because these samples had substantially worse reproducibility for $\Delta^{17}\text{O}_{\text{corr}}$ ($1\sigma = 60$ per meg, $n = 7$). Although the experimental conditions for all standard samples were identical, we used an almost-empty vial of NBS19, whereas a fresh vial of IAEA603 was opened for this experiment. We suggest that the significantly greater degree of scatter in NBS19 might be related to slight but significant exchange of this standard with moisture in this old vial, over ~ 30 years of regular use, a phenomenon discussed by other authors.²⁹

Reproducibility of $\Delta^{17}\text{O}$ was significantly improved by correction to VSMOW2-SLAP2 using eq. (3), for IAEA603 and NBS19. After correction, reproducibility of IAEA603 improved significantly from 7 per meg (1 SE) to 4 per meg; NBS19 also improved from 25 to 21 per meg. Reproducibility of NBS18 was similar before and after correction, at ~ 10 per meg. The reproducibility of our $\delta^{17}\text{O}_{\text{corr}}$ and $\delta^{18}\text{O}_{\text{corr}}$ values for IAEA603 (7 and 19 per meg, respectively), are significantly improved over previously-published TILDAS measurements of

Table 1: Triple oxygen isotope data for CO₂ evolved by phosphoric acid digestion of inter-laboratory carbonate standards at 70°C, measured by TILDAS. Between 13 and 18 aliquots were measured per sample (~ 0.9 mg total carbonate). $\delta^{17}\text{O}$ and $\delta^{18}\text{O}$ values from individual aliquots are corrected to the VSMOW2-SLAP2 scale using the IAEA603 (CO₂) and NBS18 (CO₂) values of Wostbrock et al. (2020). The corrected values, $\delta^{17}\text{O}_{\text{corr}}$ and $\delta^{18}\text{O}_{\text{corr}}$, were then used to calculate $\Delta^{17}\text{O}_{\text{corr}}$. χ_{626} is the concentration of the $^{12}\text{C}^{16}\text{O}^{16}\text{O}$ isotopologue in each sample, $\mu\text{mol}\cdot\text{mol}^{-1}$, with 1σ repeatability of aliquots in parentheses. All isotope data are ‰, with the exception of $\Delta^{17}\text{O}_{\text{corr}}$, which are per meg, $\theta = 0.528$.

Sample	χ_{626}	$\delta^{17}\text{O}^a$	$\delta^{18}\text{O}^a$	$\delta^{17}\text{O}_{\text{corr}}^b$	$\delta^{18}\text{O}_{\text{corr}}^b$	$\Delta^{17}\text{O}_{\text{corr}}$
IAEA603-4	393.3(0.5)	14.311	27.560	20.036	38.250	-158
IAEA603-5	404.8(0.6)	14.290	27.435	20.045	38.220	-140
IAEA603-6	412.8(0.8)	14.288	27.471	20.097	38.374	-161
IAEA603-7	393.8(0.8)	14.287	27.493	20.012	38.181	-147
IAEA603-9	405.3(0.7)	14.277	27.435	20.034	38.224	-149
IAEA603-10	415.6(0.7)	14.216	27.300	20.000	38.172	-158
Average		14.291	27.479	20.037	38.237	-151
$\pm 1\sigma$		0.013	0.052	0.015	0.043	10
St. err^c		0.006	0.023	0.007	0.019	4
NBS18-8	397.7(0.4)	3.605	6.925	8.941	17.148	-113
NBS18-12	409.6(0.5)	3.791	7.374	9.075	17.389	-106
NBS18-13	405.1(0.5)	3.840	7.409	9.150	17.463	-71
NBS18-14	401.8(0.9)	3.763	7.313	9.112	17.461	-107
Average		3.750	7.255	9.070	17.365	-99
$\pm 1\sigma$		0.102	0.224	0.091	0.149	19
St. err^c		0.051	0.112	0.046	0.074	10
NBS19-5	401.4(0.6)	14.164	27.295	19.895	38.052	-196
NBS19-6	409.0(0.6)	14.269	27.435	20.0533	38.266	-151
NBS19-7	397.6(0.5)	14.244	27.500	19.9783	38.222	-203
NBS19-11	397.3(0.7)	14.406	27.796	20.146	38.524	-195
NBS19-12	388.5(0.7)	14.492	27.868	20.208	38.515	-127
NBS19-13	411.3(0.5)	14.443	27.678	20.224	38.530	-120
NBS19-14	416.6(0.7)	14.418	27.798	20.184	38.582	-177
Average		14.348	27.624	20.098	38.385	-150
$\pm 1\sigma$		0.122	0.217	0.126	0.203	60
St. err^c		0.046	0.081	0.048	0.077	22

^a Molecular abundance ratios by spectroscopy, e.g. $\delta(627)$ are assumed equal to atomic abundance ratios, e.g. $\delta^{17}\text{O}$, and the atomic notation is retained; ^b Corrected using Eq. (3); ^c Standard error = $1\sigma/\sqrt{n}$

isotopologue ratios of CO₂ (reproducibilities of 30 and 40 per meg for ¹⁷O/¹⁶O and ¹⁸O/¹⁶O, respectively).^{20,21} Reproducibilities for NBS18 and NBS19 are a similar order of magnitude to these measurements. These results further emphasise the importance of correcting for scale-offset effects, at least for some samples, and provides a relatively simple strategy for correcting spectroscopic δ -values to VSMOW2-SLAP2.

Utility of high-precision $\Delta^{17}\text{O}$ (CO₂) TILDAS measurements in comparison to IRMS.

Mean $\Delta^{17}\text{O}_{\text{corr}}$ values of IAEA603, NBS18, and NBS19 by TILDAS are internally consistent with Wostbrock *et al.*,¹² and are in excellent agreement with other high-precision IRMS methods which rely on conversion of CO₂ to O₂^{9,30} to within 1 SE reproducibility (Fig. 4). Encouragingly, our methodology requires substantially less sample (~ 0.9 mg of carbonate) compared to all current IRMS methods (typically 5-10 mg).^{9,12,29,30} In addition, TILDAS requires somewhat less complicated sample preparation and shorter measurement times than IRMS.

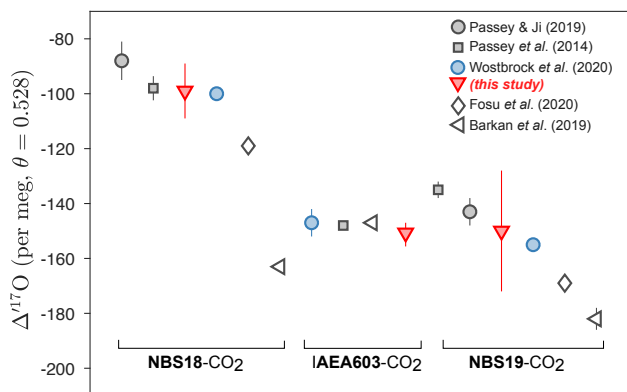


Figure 4: Comparison between TILDAS (red triangles, this study) and IRMS measurements of $\Delta^{17}\text{O}$, for CO₂ evolved from Interlaboratory Standards. Errorbars denote 1 SE. Filled grey symbols denote conversion methods (CO₂ to O₂, or direct BrF₅ fluorination of carbonate). Open symbols indicate methods reliant on platinum-catalyzed exchange of CO₂ with O₂.

One challenge of our method is the requirement that samples are very well-mixed. However, mixing the sample prior to measurement (as opposed to on a per aliquot basis), means

that the degree of mixing is easily evaluated from successive measurements of aliquot concentration(s). We also note that there is significant disagreement between some IRMS methods of triple oxygen analysis (see Fig. 4).²⁸ Typically, methods that rely on platinum-catalyzed exchange of CO₂ with O₂^{14,15,29} have systematically lower $\Delta^{17}\text{O}$ values than conversion methods. Our $\Delta^{17}\text{O}$ values are corrected to values from a conversion method, and are therefore in disagreement with exchange methods, with the exception of NBS19, which, to within its large uncertainty, agrees with most methods. Because this problem seems to be unique to our NBS19, we argue that these errors are likely related to sample heterogeneity and contamination issues (discussed above). The result underscores the importance of using carefully-chosen standards in triple oxygen isotope research, for which future interlaboratory comparison is warranted.

Conclusions

We have presented a method for triple oxygen isotope analysis by TILDAS, with a sample reproducibility for $\Delta^{17}\text{O}$ of CO₂ from interlaboratory carbonate standards that equals that of current high-precision IRMS methods (provided the sample is well-mixed in N₂). Our method brings several additional advantages, such as smaller sample size (e.g. ~ 0.9 mg of carbonate), increased throughput, and direct measurement of $\Delta^{17}\text{O}$ in CO₂. In addition, our system is readily modifiable. It is able to handle several different sources of CO₂, e.g. via Gasbench acid digestion, break-seal vials, or dry atmospheric samples collected in our removable flask (~ 586 mL). We have set out a simple procedure for the correction of TILDAS δ -values to the VSMOW2-SLAP2 scale. Future work will allow for more direct calibration via equilibration of CO₂ with VSMOW2 and SLAP2 waters, and combine TILDAS measurements of $\Delta^{17}\text{O}$ with multiply-substituted CO₂ isotopologues,¹⁹ so that $\delta^{17}\text{O}$, $\delta^{18}\text{O}$, and δ_{47} of the same sample are measured simultaneously. We expect this, or similar techniques, to have significant impact on future atmospheric monitoring and terrestrial (paleo)climate

research.

Supporting Information

Supporting Information: Additional experimental details, including photographs of experimental setup (DOC), and LabVIEW and ECL code (PDF).

Acknowledgement

This work was funded by the South African Biogeochemistry National Research Infrastructure Platform (BIOGRIP), and a Launching Grant from the University of Cape Town, as well as a grant from the National Research Foundation of South Africa (120806). VJH thanks Ben Passey and Naomi Levin for hosting him at the University of Michigan $\Delta^{17}\text{O}$ line, kindly facilitated by Tyler Faith, and Dave Braun (NSF Grant 1826666). Shuhei Ono is thanked for support and comments in the early conception of this project.

References

- (1) Thiemens, M. H.; Jackson, T.; Zipf, E. C.; Erdman, P. W.; van Egmond, C. Carbon dioxide and oxygen isotope anomalies in the mesosphere and stratosphere. *Science* **1995**, *270*, 969–972.
- (2) Boering, K.; Jackson, T.; Hoag, K.; Cole, A.; Perri, M.; Thiemens, M.; Atlas, E. Observations of the anomalous oxygen isotopic composition of carbon dioxide in the lower stratosphere and the flux of the anomaly to the troposphere. *Geophys. Res. Lett.* **2004**, *31*.
- (3) Yeung, L. Y.; Affek, H. P.; Hoag, K. J.; Guo, W.; Wiegel, A. A.; Atlas, E. L.; Schaufli, S. M.; Okumura, M.; Boering, K. A.; Eiler, J. M. Large and unexpected en-

- richment in stratospheric $^{16}\text{O}^{13}\text{C}^{18}\text{O}$ and its meridional variation. *PNAS* **2009**, *106*, 11496–11501.
- (4) Yang, J.-W.; Brandon, M.; Landais, A.; Duchamp-Alphonse, S.; Blunier, T.; Prié, F.; Extier, T. Global biosphere primary productivity changes during the past eight glacial cycles. *Science* **2022**, *375*, 1145–1151.
- (5) Hoag, K.; Still, C.; Fung, I.; Boering, K. Triple oxygen isotope composition of tropospheric carbon dioxide as a tracer of terrestrial gross carbon fluxes. *Geophys. Res. Lett.* **2005**, *32*.
- (6) Miller, M. F.; Pack, A. Why measure ^{17}O ? Historical perspective, triple-isotope systematics and selected applications. *Rev. Mineral. Geochem.* **2021**, *86*, 1–34.
- (7) Hofmann, M.; Horváth, B.; Schneider, L.; Peters, W.; Schützenmeister, K.; Pack, A. Atmospheric measurements of $\Delta^{17}\text{O}$ in CO_2 in Göttingen, Germany reveal a seasonal cycle driven by biospheric uptake. *Geochim. Cosmochim. Acta* **2017**, *199*, 143–163.
- (8) Bao, H.; Lyons, J.; Zhou, C. Triple oxygen isotope evidence for elevated CO_2 levels after a Neoproterozoic glaciation. *Nature* **2008**, *453*, 504–506.
- (9) Passey, B. H.; Hu, H.; Ji, H.; Montanari, S.; Li, S.; Henkes, G. A.; Levin, N. E. Triple oxygen isotopes in biogenic and sedimentary carbonates. *Geochim. Cosmochim. Acta* **2014**, *141*, 1–25.
- (10) Gehler, A.; Gingerich, P. D.; Pack, A. Temperature and atmospheric CO_2 concentration estimates through the PETM using triple oxygen isotope analysis of mammalian bioapatite. *PNAS* **2016**, *113*, 7739–7744.
- (11) Lehmann, S. B.; Levin, N. E.; Passey, B. H.; Hu, H.; Cerling, T. E.; Miller, J. H.; Arppe, L.; Beverly, E. J.; Hoppe, K. A.; Huth, T. E., et al. Triple oxygen isotope

- distribution in modern mammal teeth and potential geologic applications. *Geochim. Cosmochim. Acta* **2022**,
- (12) Wostbrock, J. A.; Cano, E. J.; Sharp, Z. D. An internally consistent triple oxygen isotope calibration of standards for silicates, carbonates and air relative to VSMOW2 and SLAP2. *Chem. Geol.* **2020**, *533*, 119432.
- (13) Mahata, S.; Bhattacharya, S.; Wang, C.-H.; Liang, M.-C. Oxygen isotope exchange between O₂ and CO₂ over hot platinum: An innovative technique for measuring $\Delta^{17}\text{O}$ in CO₂. *Anal. Chem.* **2013**, *85*, 6894–6901.
- (14) Fosu, B. R.; Subba, R.; Peethambaran, R.; Bhattacharya, S.; Ghosh, P. Developments and applications in triple oxygen isotope analysis of carbonates. *ACS Earth Space Chem.* **2020**, *4*, 702–710.
- (15) Barkan, E.; Musan, I.; Luz, B. High-precision measurements of $\delta^{17}\text{O}$ and $^{17}\text{O}_{\text{excess}}$ of NBS19 and NBS18. *Rapid Commun. Mass Spectrom.* **2015**, *29*, 2219–2224.
- (16) Barkan, E.; Luz, B. High-precision measurements of $^{17}\text{O}/^{16}\text{O}$ and $^{18}\text{O}/^{16}\text{O}$ ratios in CO₂. *Rapid Commun. Mass Spectrom.* **2012**, *26*, 2733–2738.
- (17) Genoud, G.; Vainio, M.; Phillips, H.; Dean, J.; Merimaa, M. Radiocarbon dioxide detection based on cavity ring-down spectroscopy and a quantum cascade laser. *Opt. Lett.* **2015**, *40*, 1342–1345.
- (18) Ono, S.; Wang, D. T.; Gruen, D. S.; Sherwood Lollar, B.; Zahniser, M. S.; McManus, B. J.; Nelson, D. D. Measurement of a doubly substituted methane isotopologue, ¹³CH₃D, by tunable infrared laser direct absorption spectroscopy. *Anal. Chem.* **2014**, *86*, 6487–6494.
- (19) Wang, Z.; Nelson, D. D.; Dettman, D. L.; McManus, J. B.; Quade, J.; Huntington, K. W.; Schauer, A. J.; Sakai, S. Rapid and Precise Analysis of Carbon Dioxide

- Clumped Isotopic Composition by Tunable Infrared Laser Differential Spectroscopy. *Anal. Chem.* **2019**, *92*, 2034–2042.
- (20) Sakai, S.; Matsuda, S.; Hikida, T.; Shimono, A.; McManus, J. B.; Zahniser, M.; Nelson, D.; Dettman, D. L.; Yang, D.; Ohkouchi, N. High-Precision Simultaneous $^{18}\text{O}/^{16}\text{O}$, $^{13}\text{C}/^{12}\text{C}$, and $^{17}\text{O}/^{16}\text{O}$ Analyses for Microgram Quantities of CaCO_3 by Tunable Infrared Laser Absorption Spectroscopy. *Anal. Chem.* **2017**, *89*, 11846–11852.
- (21) Sakai, S.; Otsuka, T.; Matsuda, S.; Sakairi, Y.; Uchida, R.; Sugahara, K.; Kano, A.; Yang, D. Subnanomolar Sensitive Stable Isotopic Determination in CO_2 by Tunable Infrared Laser Absorption Spectroscopy. *Anal. Chem.* **2022**, *94*, 6446–6450.
- (22) McManus, J. B.; Nelson, D. D.; Zahniser, M. S. Design and performance of a dual-laser instrument for multiple isotopologues of carbon dioxide and water. *Opt. Express* **2015**, *23*, 6569–6586.
- (23) Griffith, D.; Deutscher, N.; Caldow, C.; Kettlewell, G.; Riggensbach, M.; Hammer, S. A Fourier transform infrared trace gas and isotope analyser for atmospheric applications. *Atmos. Meas. Tech.* **2012**, *5*, 2481–2498.
- (24) Cohen, E. R.; Cvitaš, T.; Frey, J. G.; Holmström, B.; Kuchitsu, K.; Marquardt, R.; Mills, I.; Pavese, F.; Quack, M.; Stohner, J., et al. *Quantities, units and symbols in physical chemistry*; IUPAC, 2007.
- (25) Coplen, T. B. *Explanatory glossary of terms used in expression of relative isotope ratios and gas ratios*; IUPAC, 2008.
- (26) Rothman, L. S.; Jacquemart, D.; Barbe, A.; Benner, D. C.; Birk, M.; Brown, L.; Carleer, M.; Chackerian Jr, C.; Chance, K.; Coudert, L. e. a., et al. The HITRAN 2004 molecular spectroscopic database. *J. Quant. Spectrosc. Radiat. Transf.* **2005**, *96*, 139–204.

- (27) Kerstel, E. *Handbook of stable isotope analytical techniques*; Elsevier, 2004; pp 759–787.
- (28) Passey, B. H.; Levin, N. E. Triple oxygen isotopes in meteoric waters, carbonates, and biological apatites: implications for continental paleoclimate reconstruction. *Rev. Mineral. Geochem.* **2021**, *86*, 429–462.
- (29) Barkan, E.; Affek, H. P.; Luz, B.; Bergel, S. J.; Voarintsoa, N. R. G.; Musan, I. Calibration of $\delta^{17}\text{O}$ and $^{17}\text{O}_{\text{excess}}$ values of three international standards: IAEA-603, NBS19 and NBS18. *Rapid Commun. Mass Spectrom.* **2019**, *33*, 737.
- (30) Passey, B. H.; Ji, H. Triple oxygen isotope signatures of evaporation in lake waters and carbonates: A case study from the western United States. *EPSL* **2019**, *518*, 1–12.

Supporting Information

1. Photographs



Figure 5: Photograph of the TILDAS instrument (lasers housed inside black box), with automated valve sampling system (top), and custom-built cart for automated CO₂ extraction and dilution (below).

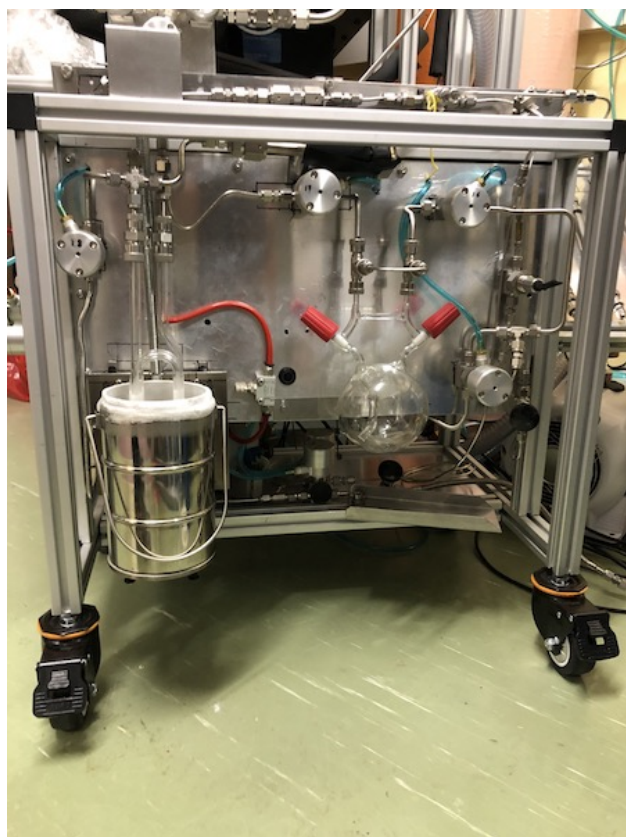


Figure 6: Photograph of the custom-built cart for automated CO₂ extraction and dilution. A pneumatically-operated dewar of liquid Nitrogen (left) is shown in the “up” position whilst CO₂ is actively trapped in MV2.



Figure 7: Photograph of MV1, the custom-built sampling flask (GlassChem cc, South Africa). Two teflon stopcocks (either Schott Produran or J. Young) seal off a ~ 586 mL round-bottomed borosilicate flask. A siphon ensures efficient flow through the volume. The flask can be disconnected from two Ultra-Torr quick connects (Swagelok). Valves 17 and 16 are shown to the left and right of the flask, respectively. A short tube of $1/8$ " diameter acts as a bypass for the flask. All other tubes are $1/4$ ". The piece of horizontal glass on the flask parallel to this bypass tube is solid, and is used to carry the flask when disconnected from the autocart. A design drawing for the flask can be obtained from the author upon request.

2. dT/dt Experiments

Summary and Results

To address the effects of temperature on TILDAS analytical precision a series of reference gas vs. reference gas experiments were conducted. Over the course of a day, repeated analyses (each with a duration between 38 and 65 minutes) of reference gas against itself were performed while varying multiple aspects of the TILDAS operational environment. In a theoretically perfect system, all $\Delta^{17}\text{O}$ values would equal 0. Tested variables were internal N_2 purge rate, lab aircon temperature setpoint, and the absence altogether of aircon temperature control, as summarized in Table A1.

Table 2: Experimental Conditions

Experiment	Time started	Duration (min)	N_2 purge (L/min)	Aircon setpoint ($^{\circ}\text{C}$)
1	6:31	65	1.5	23
2	7:38	60	1	23
3	8:59	38	1.5	23
4	10:02	60	1	23
5	11:11	45	1	23
6	12:11	57	1.5	23
7	13:31	55	1	23
8	14:34	47	1	23
9	15:30	45	1	OFF
10	16:39	41	1	24
11	17:44	52	1	OFF

Variety in the internal purge rate was not expected to have a large influence on measurement precision. Other than the potential impact on the thermal stability of the TILDAS housing, purge rate is taken to be inconsequential providing that it is sufficient to maintain a dry, N_2 dominated internal environment. As observed, the purge N_2 flow rate had negligible observable effect on analytical performance over the course of the experiments.

Several key aspects of the TILDAS system are controlled for and influenced by temperature. Laser temperatures are regulated by a liquid chiller with milli-Kelvin scale precision. The instrument used in this project uses the liquid chiller set to 23°C . As the liquid tem-

perature is maintained by a fan blowing air across the coolant liquid, lab aircon setpoint is likely to have an impact on coolant temperature stability. To ease the work load of the chiller lab aircon temperature was set to 23°C for a majority of the following experiments. The effects of lab air temperature on measurement precision were tested by occasionally shutting off the aircon unit (Experiments 9, 11) and increasing the temperature setpoint (to 24°C, Experiment 10). Previous observations not documented here revealed that an aircon setpoint matching the chiller temperature (23°C), provided greater coolant stability than a setpoint just below (22°C). However, no correlated change in measured analytical precision was observed and laser temperature stability was unaffected.

To access the impacts of electronics temperature on measurement precision, the rate of change of the temperature (dT/dt , $^{\circ}\text{C min}^{-1}$) of the electronics was mapped using a 200-second moving average. The curve produced from this moving average was plotted alongside calculated $\Delta^{17}\text{O}$ values for each measured reference gas vs. reference gas measurement cycle. A clear trend is observed correlating the amplitude (A) of the dT/dt moving average curve, hereafter $A(dT/dt)$, to measured $\Delta^{17}\text{O}$ standard deviation (1σ) (Figure A1). The outlier in the trend is the direct result of an intentional disruption to the experimental run (Experiment 5) in which the cooling fan intake on the TILDAS computer was blocked with a sheet of paper for ~ 6 minutes during the run.

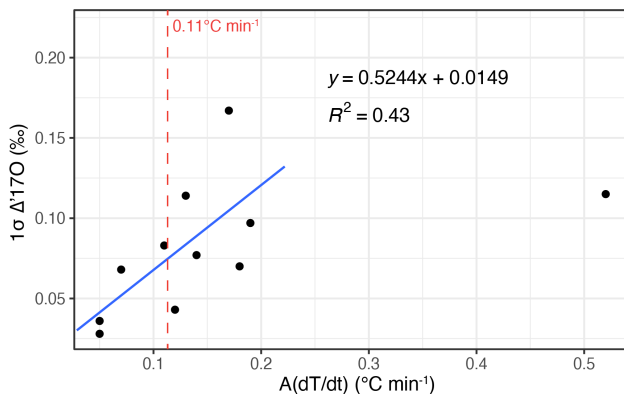


Figure 8: TILDAS electronics $A(dT/dt)$ vs. $1\sigma \Delta^{17}\text{O}$

For the system used in this project, it was realized that minimizing $A(dT/dt)$ is the

most important factor in producing high-precision $\Delta^{17}\text{O}$ measurements. To this end, it is best to perform analyses when there is no lab aircon control and the room is allowed to slowly heat up over the course of a measurement (Experiments 9 and 11). While the absolute temperature of the electronics typically increases by several degrees when applying this strategy, the continuous but consistent heating minimizes drastic instantaneous changes in dT/dt and therefore $A(dT/dt)$. Other, perhaps more practical long-term solutions to limit $A(dT/dt)$ could be the extension of the liquid cooling system to include more sensitive electronic components, adding a heat exchanger near the computer's cooling fan intake, or using a high quality aircon with PID control to continuously supply the lab space around the TILDAS with air of consistent temperature.

In summary, the results of the experiments suggest the main control over measurement precision to be dT/dt of the TILDAS electronics. The internal purge rate and absolute temperature of the electronics had little to no influence on the measured $\Delta^{17}\text{O}$ values, while the lab aircon temperature setting exerts its largest influence when set higher than the liquid chiller temperature. As the TILDAS system is constantly measuring and making corrections to adapt to its operational environment, it follows that rapid changes will exert a greater influence on instrument stability. Minimizing large instantaneous electronics temperature changes is key to achieving the necessary precision for relevant earth surface triple oxygen isotope studies using TILDAS.

Experimental setup and details

The first experiment began at 6:31am and lasted 66 minutes. Being the first analysis of the day the internal volume of the TILDAS instrument would have been equilibrated with bulk lab air both thermally and in its constituents. In an attempt to refresh the volume more quickly with dry N_2 , the internal purge rate was set to approximately 1.5L/min. The observed positive trend in $\Delta^{17}\text{O}$ values over the course of this run is assumed to be a result of the stabilizing of the instrument's internal environment.

Table 3: Summary of Results

Experiment	A(dT/dt) ^a	Avg. $\Delta^{17}\text{O}$	1σ $\Delta^{17}\text{O}$
1	0.19	-0.061	0.097
2	0.18	0.036	0.070
3	0.14	-0.004	0.077
4	0.12	-0.005	0.043
5	0.52	-0.007	0.115
6	0.13	-0.043	0.114
7	0.07	0.026	0.068
8	0.11	-0.005	0.083
9	0.05	0.017	0.036
10	0.17	0.003	0.167
11	0.05	-0.031	0.082

^a °C min⁻¹

The second experiment started at 7:38am and lasted 60 minutes. During this run, the internal purge rate was set at $\sim 1\text{L}/\text{min}$ – the setting most commonly used for sample measurements prior to, and since, these experiments. While measurement 1σ precision improved slightly to 0.070‰ , it is difficult to say whether the improvement was due to the different purge rate or simply a result of a more stable measurement environment.

The third experiment started at 8:59am and lasted 38 minutes. This experiment again tested the higher N_2 purge rate of $\sim 1.5\text{L}/\text{min}$. The experiment resulted in a $\Delta^{17}\text{O}$ 1σ precision of 0.077‰ , similar to the previous under a lower purge flow regime, with the absolute $\Delta^{17}\text{O}$ value, -0.004‰ , being within error. This experiment lends support towards the purge rate being a small factor in $\Delta^{17}\text{O}$ precision.

The fourth experiment started at 10:02 and lasted 60 minutes. The parameters for this experiment were setup identically to that of the second. The largest difference in operating conditions between this experiment and each of the previous (and ultimately from all of the following) experiments was simply the number of people in the instrument room. During this experiment, 10 individuals spent notable amounts of time in the instrument room, as compared to 1-3 for the previous runs. The high traffic during this run caused the room’s aircon to activate more frequently. This is observed in the decreased A(dT/dt) (as a result of less efficient cooling, i.e., decreased instantaneous cooling) and manifests in the nearly

halving of $\Delta^{17}\text{O}$ standard deviation (1σ) from the previous experiments to 0.043‰ with an average $\Delta^{17}\text{O}$ of -0.005‰.

The fifth experiment started at 11:11am and lasted 45 minutes. This experiment is marked by the covering of the TILDS computer cooling fan intake for ~ 6 minutes beginning at $\sim 11:40$ am. The intent behind this action was to create an immediate, drastic change to the electronics environment to assess the impacts of temperature in real time. The resulting dT/dt moving average curve from this action is a large double peak ($A(dT/dt) = 0.52^\circ\text{C min}^{-1}$), the first of which is the rapid heating of the electronics when cooling air was cut off, and the second when the fan intake was uncovered, causing rapid cooling of the electronics. While the analysis resulted in good accuracy ($\Delta^{17}\text{O} = -0.006\text{‰}$) this experiment resulted in an overall $\Delta^{17}\text{O}$ (1σ) of 0.115‰.

The sixth experiment started at 12:11am and lasted 57 minutes. This experiment was run under the higher N_2 purge flow $\sim 1.5\text{L/min}$. Overall $\Delta^{17}\text{O}$ 1σ precision was 0.114‰ and observably decreased throughout the run, correlated with inconsistent dT/dt peak frequency. There is no clear singular cause for this pattern.

The seventh experiment started at 13:31 and lasted 55 minutes. This experiment was run at the preferred N_2 purge flow $\sim 1\text{L/min}$. For unclear reasons, electronics temperature stability was improved as evidenced by the decreased $A(dT/dt)$ of $0.07^\circ\text{C min}^{-1}$. This marked the first experiment to achieve a $A(dT/dt) < 0.1^\circ\text{C min}^{-1}$. Despite this, the $\Delta^{17}\text{O}$ 1σ of 0.068‰ is not markedly improved relative to previous runs. The reason for this poorer than expected precision given the improved dT/dt profile is unclear.

The eighth experiment started at 14:34 and lasted 47 minutes. The experiment's setup was identical to the previous. $A(dT/dt)$ of $0.11^\circ\text{C min}^{-1}$ and $\Delta^{17}\text{O}$ 1σ precision of 0.083‰ are both expectedly similar to many of the previous experiments.

The ninth experiment started at 15:30 and lasted 45 minutes. The purge rate again was set to $\sim 1\text{L/min}$. This experiment is the first to test how the absence of aircon temperature control influenced measurement precision. The absolute temperature of the electronics in-

creased $\sim 3^\circ\text{K}$, roughly 3 times the temperature range observed in all previous experiments when lab aircon was in use. However, 1σ $\Delta^{17}\text{O}$ precision was 0.036‰ and correlated to a low $A(dT/dt)$ of $0.05^\circ\text{C min}^{-1}$, each of which are respectively the lowest of any experiment thus far. This experiment is a clear improvement in creating ideal measurement conditions and shows that absolute electronics temperature is not a major control on measurement precision.

The tenth experiment started at 16:39 and lasted 41 minutes. A N_2 purge rate of $\sim 1\text{L/min}$ is maintained. This experiment tested setting lab aircon setpoint to 24°C , higher than the liquid chiller setpoint, to test the effects of potentially inconsistent cooling on the system. This experiment resulted in a high $A(dT/dt)$ of $0.17^\circ\text{C min}^{-1}$ and a correspondingly poor $\Delta^{17}\text{O}$ 1σ of 0.167‰ – by far the worst precision observed in this series of experiments. The electronics temperature profile is markedly different than previous experiments with aircon control, characterized by decreased regulation frequency and a larger absolute range.

The eleventh and final experiment started at 17:44 and lasted 52 minutes. Again a $\sim 1\text{L/min}$ N_2 purge rate is used. This experiment again tested the absence of lab aircon control on measurement precision, with similarly good results. Absolute electronics temperature increased $\sim 3^\circ\text{K}$ with a similar profile to that of Experiment 9. The $\Delta^{17}\text{O}$ 1σ of 0.028‰ is the best achieved in any of the experiments performed. The low $A(dT/dt)$ of $0.05^\circ\text{C min}^{-1}$ matches that of experiment 9 in which lab aircon was also not used. While the $\Delta^{17}\text{O}$ value of -0.031‰ is not within measurement error of the theoretical value of 0.000‰ , the improvement of measurement precision is encouraging.

3. Labview code

All LabVIEW code, and TDLWintel ECL scripts can be found on github, here:

<https://github.com/vinhare/UCT-TILDAS-17O>

Please cite as:DOI :10.5281/zenodo.6802227

AutoCart LabVIEW valves, volumes, and sample sequences

Mixing volumes

Mixing volume 1 (MV1) – 586mL (flask + V16-V17 volume)

Mixing volume 2 (MV2) – 61mL (liquid N₂ trap)

Mixing volume 3 (MV3) – 40mL (bellows)

AutoCart valves

V1 (diaphragm valve) – Up-stream end of cracker 1

V2 (diaphragm valve) – Up-stream end of cracker 2

V3 (diaphragm valve) – Up-stream end of cracker 3

V4 (diaphragm valve) – Down-stream end of cracker 1

V5 (diaphragm valve) – Down-stream end of cracker 2

V6 (diaphragm valve) – Down-stream end of cracker 3

V7 (diaphragm valve) – Inlet for N₂ supply

V8 (3-way solenoid valve) – N₂ supply director (normally open to break-seal manifold, normally closed to V21/MV3)

V16 (diaphragm valve) – Separates sample inlet side from preparation side of AutoCart

V17 (diaphragm valve) – Separates flask volume from liquid N₂ trap

V18 (diaphragm valve) – Separates liquid N₂ trap from MV3

V19 (diaphragm valve) – Inlet from AutoCart to TILDAS switching valve system

V20 (diaphragm valve) – To vacuum pump

V21 (diaphragm valve) – Dilution N₂ shut-off

Circulation Loop (2x diaphragm valve) – 2 pneumatically connected valves at either end of the circulation loop

Manual toggle valve separating GasBench system & AutoCart

Manual twist valve separating cracker manifold & AutoCart

Carbonate samples from GasBench

- Reset all sample data values to 0
- Open V7
- Open V16
- User input – close off flask via stopcocks
- Open circulation loop and pump out for 60 seconds
- Open V8 – Switch N₂ direction to V21/MV3
- Close V20
- Open V21
- Pressurize circulation loop to 1300 mbar
- Close V21
- Briefly (1-2 seconds) circulate dry N₂ through loop via diaphragm pump
- Close circulation loop
- Close V8 – Switch N₂ direction away from V21/MV3
- Open V20 – pump system down to <76 mtorr
- Close manual valve connecting AutoCart to cracker manifold
- Open manual valve connecting GasBench system to AutoCart
- Pump out GasBench capillary for 30 seconds
- Raise liquid N₂ dewar and allow liquid N₂ trap to cool
- Manually restrict flow from vacuum pump to AutoCart via twist valve
- Use GasBench sampling needle to direct sample gas through the GasBench and to the AutoCart
- 40-minute sample transfer wait time
- Direct GasBench system away from AutoCart
- Pump AutoCart to <75 mtorr
- Close V16
- Close V17
- Close V18

- Close manual valve connecting GasBench system to AutoCart
- Remove liquid N₂ dewar from trap
- Allow 6 minutes for sample to thaw
- Read thaw pressure and calculate $\mu\text{mol CO}_2$ trapped and dilution requirements
- Open left flask stopcock to allow sample into flask (MV1)
- Open V17 – expand sample into flask 40 seconds
- Close V17
- Close V20
- Open V8 – Switch N₂ direction towards V21/MV3
- Open V21 – build N₂ pressure in MV3 for 30 seconds
- Open V18
- Begin turbulent mixing steps – repeat n times as determined by measured CO₂ yield
 - Pressurize MV3 + MV2 to 1450 mbar
 - Open V17
 - 5 second expansion into MV1
 - Close V17
- If turbulent mixing steps don't achieve required P, N₂ is added non-turbulently until necessary pressure (Dilution Target Pressure) is reached
- Close V17
- Close V8 – Switch N₂ direction away from V21/MV3
- Close V21
- Open V20
- Pump out leftover N₂ from MV3 + MV2 for 2 minutes
- Close V20
- Open V17 – expand diluted sample from MV1 through MV2 + MV3
- Measure sample final pressure
- Open V16

- Open circulation loop valves turn on diaphragm pump for 150 seconds
- Close circulation loop valves turn off diaphragm pump
- Close V16
- Open V19 and begin TILDAS analysis

Break-seal samples from AutoCart mount

Written for samples from break-seal 1 (2) (3)

- Reset all sample data values to 0
- Open V7
- Open V16
- Close V5 (4) (4)
- Close V6 (6) (5)
- User input – close off flask via stopcocks
- Close both manual valves connecting AutoCart to cracker manifold and GasBench
- Open circulation loop and pump out for 60 seconds
- Open V8 – Switch N₂ direction towards V21/MV3
- Close V20
- Open V21
- Pressurize circulation loop to 1300 mbar
- Close V21
- Briefly (1-2 seconds) circulate dry N₂ through loop via diaphragm pump
- Close circulation loop
- Close V8 – Switch N₂ direction away from V21/MV3
- Open V20
- Open manual valve connecting cracker manifold to AutoCart
- Open V4 (5) (6)

- Pump system down to <76 mtorr
- Raise liquid N₂ dewar and allow liquid N₂ trap to cool
- Close V18
- Break break-seal containing sample
- Allow 10 minutes for cryo-pull trapping of sample CO₂
- Open V18
- Pump over frozen sample to <75 mtorr
- Close V17
- Close V18
- Close V16
- Close V4 (5) (6)
- Remove liquid N₂ dewar from trap
- Allow 6 minutes for sample to thaw
- Close manual valve connecting AutoCart to cracker manifold
- Open left flask stopcock to allow sample into flask (MV1)
- Read thaw pressure and calculate $\mu\text{mol CO}_2$ trapped and dilution requirements
- Open V17 – expand sample into MV1 for 40 seconds
- Close V17
- Close V20
- Open V8 – Switch N₂ direction towards V21/MV3
- Open V21 – build N₂ pressure in MV3 volume for 30 seconds
- Open V18
- Begin turbulent mixing steps – repeat n times as determined by measured CO₂ yield
 - Pressurize MV3 + MV2 to 1450 mbar
 - Open V17
 - 5 second expansion into MV1
 - Close V17

- If turbulent mixing steps don't achieve required P, N₂ is added non-turbulently until necessary pressure (Dilution Target Pressure) is reached
- Close V17
- Close V8 – Switch N₂ direction away from V21/MV3
- Close V21
- Open V20
- Pump out leftover N₂ from MV3 + MV2 for 2 minutes
- Close V20
- Open V17 – expand diluted sample from MV1 through MV2 + MV3
- Measure sample final pressure
- Open V16
- Open circulation loop valves turn on diaphragm pump for 150 seconds
- Close circulation loop valves turn off diaphragm pump
- Close V16
- Open V19 and begin TILDAS analysis

Atmospheric flask samples

- Start assuming flask has been replaced inline on AutoCart and headspace evacuated
- Reset all sample data values to 0
- Open V7
- Open V16
- Close manual valve connecting cracker manifold to AutoCart
- Close manual valve connecting GasBench system to AutoCart
- Open circulation loop and pump out for 60 seconds
- Open V8 – Switch N₂ direction to V21/MV3
- Close V20
- Open V21
- Pressurize circulation loop to 1300 mbar

- Close V21
- Briefly (1-2 seconds) circulate dry N₂ through loop via diaphragm pump
- Close circulation loop
- Close V8 – Switch N₂ direction away from V21/MV3
- Open V20 – pump system down to <76 mtorr
- Close V16
- Close V17
- Open flask stopcocks to open sample to V16-17 volume (MV1)
- Raise liquid N₂ dewar and allow liquid N₂ trap to cool
- Manually restrict flow from vacuum pump to AutoCart via twist valve
- Open V17
- Pump flask through liquid N₂ trap to < 90 mtorr
- Close V17
- Close V18
- Remove liquid N₂ dewar from trap
- Allow 6 minutes for sample to thaw
- Read thaw pressure and calculate $\mu\text{mol CO}_2$ trapped and dilution requirements
- Open left flask stopcock to allow sample into flask (MV1)
- Open V17 – expand sample into flask 40 seconds
- Close V17
- Close V20
- Open V8 – Switch N₂ direction towards V21/MV3
- Open V21 – build N₂ pressure in MV3 volume for 30 seconds
- Open V18
- Begin turbulent mixing steps – repeat n times as determined by measured CO₂ yield
 - Pressurize MV3 + MV2 to 1450 mbar
 - Open V17

- o 5 second expansion into MV1
- o Close V17
- If turbulent mixing steps don't achieve required P, N₂ is added non-turbulently until necessary pressure (Dilution Target Pressure) is reached
- Close V17
- Close V8 – Switch N₂ direction away from V21/MV3
- Close V21
- Open V20
- Pump out leftover N₂ from MV3 + MV2 for 2 minutes
- Close V20
- Open V17 – expand diluted sample from MV1 through MV2 + MV3
- Measure sample final pressure
- Open V16
- Open circulation loop valves turn on diaphragm pump for 150 seconds
- Close circulation loop valves turn off diaphragm pump
- Close V16
- Open V19 and begin TILDAS analysis

Sequence summary

Each of the 3 sequence types handled by the LabVIEW code can be summarized by being split into three parts. For each of them, the first part is preparation of the circulation loop later used for mixing the diluted sample gas, the second part cryo-trapping and pumping over of the sample gas, and the third part, which is identical for all sequences and sample types, is the thawing, diluting, and mixing of the sample gas. Following is a summary of the sample preparation sequences currently incorporated in the LabVIEW code. Information regarding valve type, mixing volumes, and step by step breakdowns for each of the sequences can be found in the supplementary file "AutoCart LabVIEW valves, volumes, and sample

sequences".

Preparing the circulation loop happens identically for all sample sequences. First, the loop is manually evacuated then filled with high purity N_2 to 1100 mbar. The sequence is then started, the first steps being the re-evacuation of the loop and subsequent pressurizing to 1300 mbar of the same high-purity N_2 . The inline diaphragm pump is then briefly activated to cycle gas through the loop, moving any potential atmosphere leak during evacuation into a more easily evacuated volume and recharging the loop with N_2 . The circulation loop is then closed off on either end and allowed to slowly leak N_2 during the duration of the respective sample preparation sequences.

The preparation sequences differ in the sample transfer, cryo-trapping, and post-trapping cleaning steps. Carbonate samples introduced via the GasBench II are manually sampled via the sampling needle and directed into the AutoCart upstream of MV1. The CO_2 passes over the flask via a bypass as the flask valves are closed at this point and is cryo-trapped in MV2. A transit time of 40 minutes is allotted for comprehensive transfer and collection of sample CO_2 from the sampling vials. MV2 is the vacuum pumped over the frozen sample gas to 75 mTorr before sample thaw.

Samples introduced via break-seals on the cracker manifold are cryo-pulled under static vacuum into MV2 for 10 minutes, passing over the flask via the same bypass. After 10 minutes, the full volume is vacuum pumped over the frozen sample gas to 75 mTorr before sample thaw.

Atmospheric samples introduced by connecting the sampling flask to the AutoCart as MV1 are handled initially by evacuating the MV1 head-space created. Once evacuated, MV1 is closed off at valves 16 and 17 and the flask valves opened. The sample is then restrictively vacuum pumped through the cryo-trap on MV2 to 90 mTorr. Once achieved, the sample is thawed in MV2. This process typically takes ~ 50 minutes. It is of suspicion that a small amount of atmospheric N_2 condenses in the cryo-trap during this process. This excess gas is accounted for by a small offset in the sample yield when calculating dilution specifications.

For all sequences samples are allowed to thaw for 6 minutes in MV2 before the yield is measured. Measured yields are then used to calculate sample dilution requirements including amount of N₂ to be added and the number of turbulent mixing steps to be performed. The sample CO₂ is expanded into MV1 and signifies the beginning of the dilution and mixing process.

Sample dilution and initial mixing takes place in MV1 and is done by repeatedly pressurizing MV3 and MV2 to 1450 mbar of N₂ and subsequently expanding into MV1. The large pressure change combined with the flask's specific design to maximize turbulence promote even sample dilution. After pressure equilibration, MV1 is isolated and MV3 and MV2 repressurized to 1450 mbar. These steps are repeated n times as determined by measured sample yield (typically 4-5). n is calculated according to the curve $n = 3e^{-6x^2} + 0.0031x + 0.0261$, where x is the target dilution pressure. n need not strictly be rounded to a whole number but can be a decimal under the condition that the fraction of n multiplied by 1450 mbar is greater than the pressure already contained in MV1 after the previous expansion. For example, when $n = 4.872$, $0.872 \times 1450 \text{ mbar} = 1264.4 \text{ mbar}$. Typical MV1 pressure after 4 expansions is $\sim 765 \text{ mbar}$, so an expansion of 1264.4 mbar would occur to complete sample dilution. In the event that a partial expansion cannot occur (e.g. when $n = 4.123$, $0.123 \times 1450 \text{ mbar} = 178.4 \text{ mbar}$, less than MV1 pressure), n is rounded down to the nearest whole number and N₂ is then non-turbulently added to MV1 via valve V21 until the calculated dilution pressure is reached.

The direction of N₂ flow from MV3 through MV2 and into MV1, combined with the earlier expansion of the sample CO₂, concentrates the sample in MV1. This causes an excess of N₂ in MV2 and MV3 at the end of the dilution process. To overcome this, dilution requirements are calculated with respect to MV1 (586mL) rather than the combined volume of MV1,2,3 (687 mL). After the dilution process is complete, V17 closes, isolating MV1, and MV2 and MV3 are evacuated. MV1 is then expanded to MV1,2,3, thereby achieving accurate sample dilution throughout the entirety of the mixing volumes where true dilution

pressure and accuracy are recorded.

Further mixing occurs as the circulation loop is opened to the full mixing volume and the diaphragm pump activated. The diaphragm pump circulates at 750mL/min for 2.5 minutes, allowing sample gas to circulate through the entirety of the cart ~ 3 times. After 2.5 minutes of circulating the diaphragm pump is switched off, the loop is closed, and sample preparation is considered complete.